

SUPPLEMENTARY MATERIAL

Where are the coexisting parallel climates?

Large ensemble climate projections from the point of view of chaos theory

M. Herein, T. Tél, T. Haszpra

S1. ILLUSTRATIVE CLIMATE AND CHAOS MODELS

The CESM1-LE climate model. We use the data of one of the notable and widely studied SMILEs, the CESM1-LE produced by the fully coupled CESM1 used in CMIP5. CESM1-LE was designed with the very explicit goal to measure the internal variability of the climate system in the presence of forced climate change on the time scale of a few centuries. All realizations arise from CESM1 with the Community Atmosphere Model, version 5 (Hurrell et al., 2013) at a resolution of 192 x 288 in latitudinal and longitudinal directions, with 30 atmospheric levels. CESM1-LE uses ocean [Parallel Ocean Program, version 2 (POP), 60 vertical levels], land [Community Land Model, version 4 (CLM4)], and sea ice [Los Alamos Sea Ice Model (CICE)] component modules, coupled via a coupler module to the dynamic atmosphere (for details see Kay et al., 2015). A previously generated steady state preindustrial control run is used as the initial condition for the first member of CESM1-LE. This first member uses initial conditions of a randomly selected date in 1850 run for 400 years to reach a steady state. Afterwards, it is integrated forward to 2100 with the standard CMIP5 forcing protocol using observed data between 1850 and 2005, while from 2006 to 2100 the RCP8.5 protocol is applied (Lamarque et al., 2010; Taylor et al., 2012; Meinshausen et al., 2011; Van Vuuren et al., 2011). All the other CESM1-LE members (2-40) derive from this first member by perturbing it in the air temperature field at the beginning of the year 1920, which yields the starting point of the whole ensemble with all members subjected to the same forcing as the first one. We utilized the daily and monthly global mean surface temperature for all realizations for time interval 1920-2021. The global daily mean surface temperature was determined by using the Climate Data Operators software (CDO, Schulzweida, 2021). From monthly data we calculated, using CDO, the time evolution of the global annual mean surface temperature (TS) from 1920 to 2021.

Considering the convergence time estimated to be $t_c = 40$ years by Bódai et al. (2020), we note that this time corresponds to that set by the atmosphere and the upper ocean only, and not

33 the one set by the deep ocean, which has a time scale of at least hundreds or thousands of years
 34 (Vallis, 2017; Drótos and Bódai, 2022). It is worth recalling that a control run is used to reach
 35 a quasi-stationary state relevant for 1850 (preindustrial conditions). This means that the deep
 36 ocean has had time to converge to a quasi-stationary state (Kay et al., 2015). It is therefore
 37 sufficient to skip the afore-mentioned first 40 years of the realizations; thus, the simulated
 38 results can be considered to represent a converged ensemble, and thus climate, appropriately,
 39 from 1960 onward. We also note that other models might possess, of course, different
 40 convergence times, t_c , see e.g., Branstator and Teng (2010), Pierini (2020).

41 For comparison with measurements, we use Met Office Hadley Centre’s latest
 42 recommended observations dataset HadCRUT5 (Morice et al., 2021). The climatology from
 43 1961-1990 (global historical surface temperature relative to a 1961-1990 reference period) is
 44 used to obtain the global mean surface temperature record.

45

46 *The chaos model.* From a broad class of typical low-dimensional chaotic models, the only
 47 feature important for the comparison is the presence of a time-periodic driving, mimicking, e.g.,
 48 the annual cycles of the climate. As such an example, we consider a driven dissipative
 49 pendulum whose suspension point is periodically moving along a horizontal line. Its equation
 50 of motion is given as (see Tél and Gruiz 2006):

$$51 \quad \dot{\varphi} = \omega, \quad (1)$$

$$52 \quad \dot{\omega} = -a \cdot \omega - g/l \cdot \sin(\varphi) + A/l \cdot \omega^2 \cdot \cos(\Omega t) \cdot \cos(\varphi), \quad (2)$$

53 where φ and ω are the angle (relative to the vertical) and angular velocity, respectively, and Ω
 54 represents the frequency of the driving. As an illustrative chaotic parameter set we take $l = 1$ m
 55 as the length of the pendulum, $A = 2$ m and $\Omega = 9.5$ Hz the amplitude and frequency,
 56 respectively, of the horizontal oscillation of the suspension point, while $a = 0.95$ 1/s is the
 57 damping constant, and we use $g = 9.8$ m/s² for the gravity of Earth. The driving period is thus
 58 $2\pi/\Omega = 0.66$ s. We note that the dynamics remains very similar for a broad choice of parameters.

59

60 **S2. CONVERGENCE AND SIZE-DEPENDENCE OF ENSEMBLE** 61 **RESULTS**

62

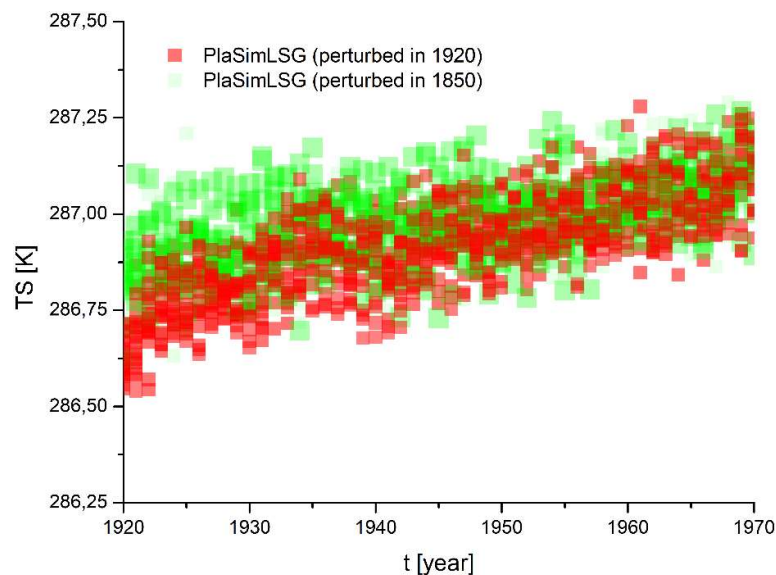
63 *Planet Simulator (Plasim)* is a freely available intermediate complexity climate model
 64 (Fraedrich et al., 2005; Lunkeit et al., 2011) which we use to simulate aspects of Earth’s climate
 65 which are not accessible via CESM1-LE for us. PlaSim was developed to understand the main

66 physical processes in climate dynamics. In previous studies (see, e.g. Lucarini et al., 2010,
67 Herein et al., 2017, Kilic et al., 2018, Vincze et al., 2021) it proved to be an appropriate
68 numerical tool to investigate certain global aspects of the climate system. For our purposes, we
69 make use of the same atmospheric setup as in Lucarini et al. (2010). As a non-standard aspect
70 of our model setup, the PlaSim atmosphere is coupled to a large scale geostrophic (LSG) ocean
71 (The Hamburg Large Scale Geostrophic Ocean General Circulation Model (Cycle 1) Maier-
72 Reimer, 1991). We use the default resolution of $3.5^\circ \times 3.5^\circ$ and 22 non-equidistant vertical
73 layers along with a realistic present-day bathymetry. We note that the LSG ocean is spun up
74 over a period of 10000 years to reach steady state.

75

76 **Converged ensembles.** We emphasize that not waiting until a convergence occurs to the
77 climate attractor may have a remarkable effect on the behaviour of any ensemble climate model
78 (Drótos et al., 2017; Drótos and Bódai, 2022), and might be the reason that the CESM1-LE
79 differs from the observations in the first 20 years of the simulation (Fig. 2). With PlaSim, we
80 run two 20-member ensemble simulations with the very same forcing but with different
81 initializations. After a single steady state run, which is converged to the preindustrial climate
82 state of 1850 ($\text{CO}_2=278$ ppm) we follow the historical forcing (Taylor et al., 2012; Lamarque
83 et al., 2010). However, from 1958 onward we use the available measured data (Keeling et al.,
84 2001) up to 1970.

85



86

87 Fig. S1. Illustrating the importance of the convergence. Climate model PlaSim with identical forcing
88 scenarios but with two different ensemble initializations. Red color shows variable TS for a 20-member
89 ensemble initialized in 1920, while green indicates an ensemble with the same size initialized in 1850,
90 which can be considered as converged by 1920.

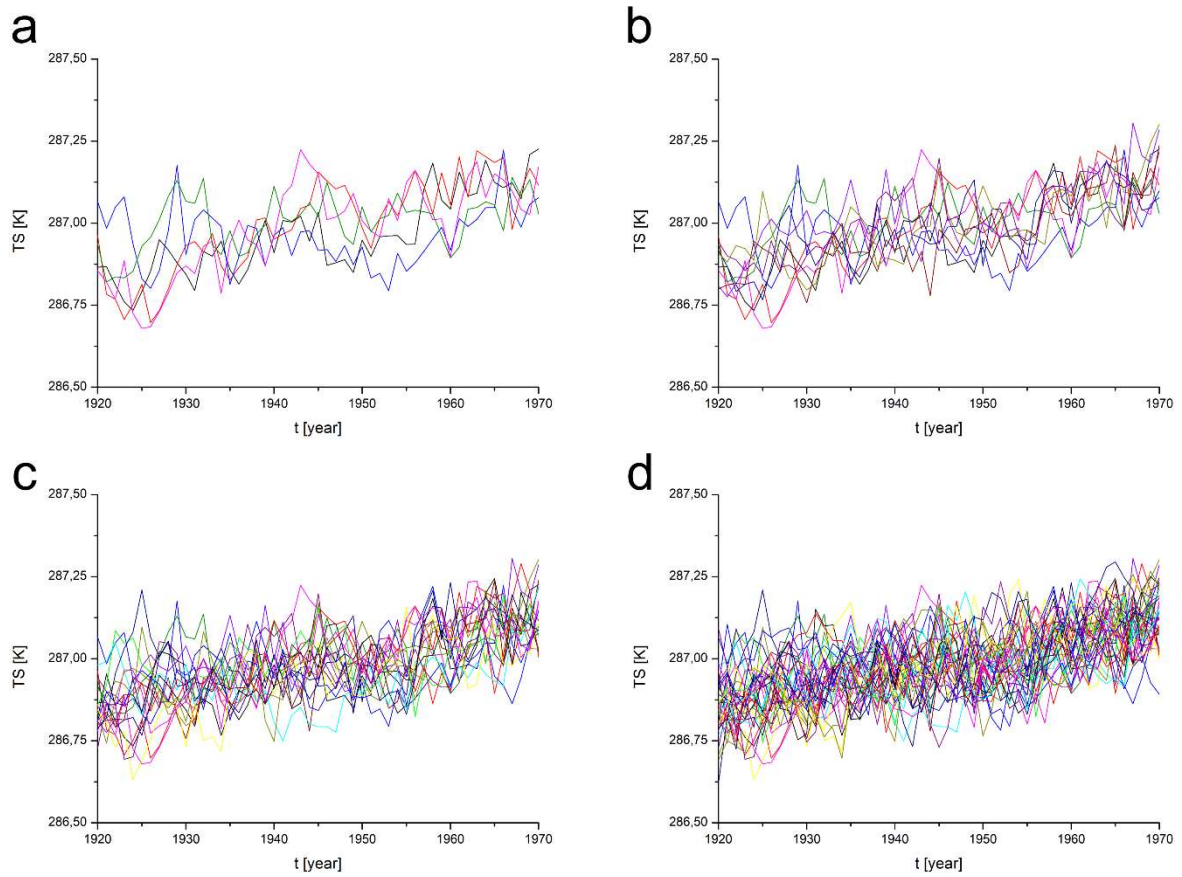
91

92 All the members of the first ensemble are initialized in 1850 with a slight random
93 perturbation of the surface pressure (of the order of 10^{-4} Pa) and integrated up to 1970 (Fig. S1
94 green dots). The second ensemble originates from a single run, started in 1850, by perturbing it
95 in a similar way as the first ensemble, just in 1920, to generate a 20-member ensemble (Fig. S1
96 red dots). We mention that this second technique is very similar to CESM1-LE's initialization,
97 however, instead of temperature we use a pressure perturbation. By 1920, 70 years after
98 initialization, the green ensemble can be considered to be a converged one. In Fig. S1 one sees
99 clearly that there is a definite time needed for the red ensemble to reach the green one, i.e. the
100 red ensemble can be considered converged. The convergence time is approximately $t_c=30$ years
101 in this case. This means that the red ensemble can be viewed identical to the green one after 30
102 years only. In other words, the red one is not relevant for climate in the first 30 years of the
103 simulation. The value of the convergence time being approximately 30 years is consistent with
104 the finding of Drótos et al. (2017).

105

106 *Effect of the ensemble size.* We illustrate in PlaSim that the spread is practically
107 constant for sufficiently large ensembles. Note that the size of the spread cannot grow arbitrarily
108 since it is determined by a chaotic-like dynamics whose variance is always finite. In low-order
109 models this corresponds to the fact that the size of chaotic attractors is typically finite in all
110 directions (Tél and Gruiz, 2006). In Fig. S2 an optical impression is given about the size
111 dependence by plotting all ensemble members of the converged, green ensemble of Fig. S1 in
112 the period 1920-1970 for $N = 5, 10, 20, 40$. In the last two cases the spread hardly changes with
113 N and proves to be approximately constant in time, as also illustrated via another representation
114 in Fig. S3. This observation reinforces the statement by Milinski et al. (2020) and Pierini (2020)
115 according to which the ensemble size of a few times ten appears to be sufficient.

116



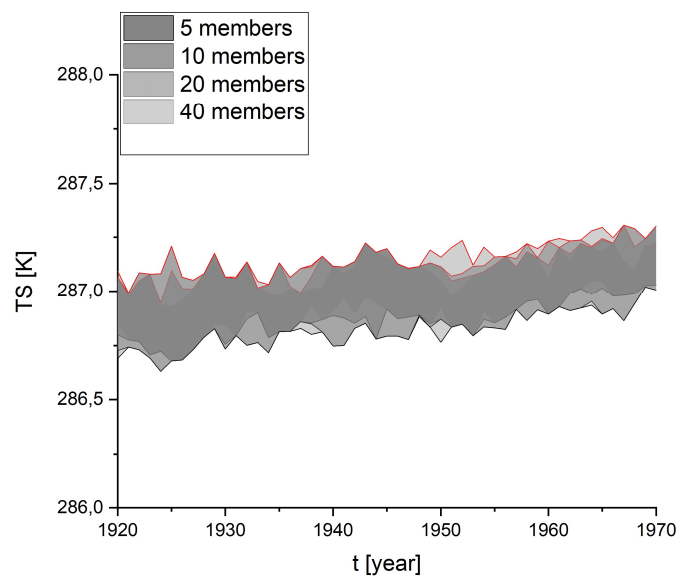
117

118

119

120

Fig. S2. Parallel climate realizations in PlaSim from 1920 to 1970 for TS for ensembles of size $N=5$, 10, 20, and 40 in panels (a), (b), (c) and (d), respectively.



121

122

123

124

125

126

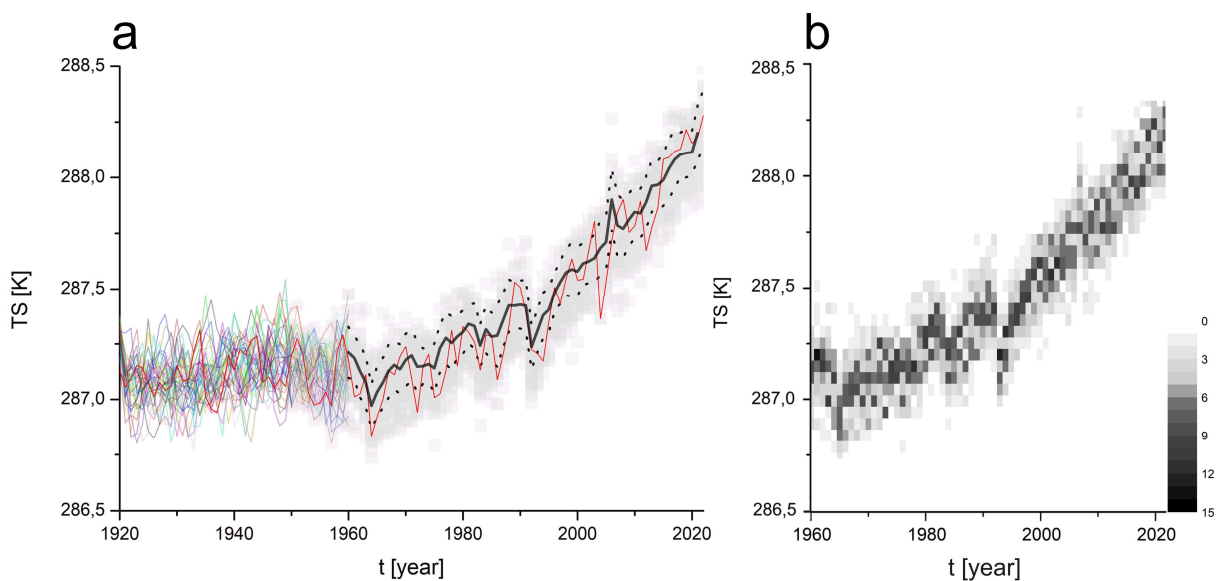
Fig. S3. The size-dependence of the spread in Plasim for variable TS in the green ensemble of Fig. S1. The spreads represented by different shades of grey (see legend) are overlaid on each other with the darkest shade in the topmost layer.

127 **S3. PROPERTIES OF CONVERGED ENSEMBLES**

128

129 Returning to CESM1-LE, in Fig. S4a one of the realizations, the first member of the
130 ensemble, is also plotted, in red, through the full investigated period. One clearly sees that this
131 curve often exits the region between the dotted lines, and is thus *not representative* for the
132 ensemble. In fact, none of the individual simulations is. The character of the red curve is,
133 however, similar to that of the blue one in Fig.2, illustrating that the measured time series should
134 behave as an individual ensemble member if the simulation is credible.

135



136

137 Fig. S4. (a) Similar to Fig.2 (a), but the first member of the CESM1-LE ensemble is also plotted
138 throughout the full interval (red curve) (instead of the measured dataset, the blue curve in Fig.2 (a)). (b)
139 Time dependent distribution of the frequency of the occurrence of a given temperature (number of TS
140 values falling in a bin of 0.05 K and of the lengths of one year). Fig. 2 (b) of the main text is a smoothed
141 version of Fig. S4 (b) for a more aesthetic visual impression. Darker shadings indicate higher “frequencies”
142 as the legend shows.

143

144 It is the full *probability distribution* set by the ensemble which is a characteristic of the
145 climate, two important measures of which are the mean and the standard deviation (see e.g. Ott,
146 2006; Drótos and Bódai, 2022). To represent the full probability distribution provided by the
147 ensemble, in Fig.S4b shading is applied proportional to the number of realizations falling into
148 a bin of the above-mentioned size of 0.05 K. Darker areas mark higher numbers. This is not at
149 all in contradiction with the unpredictability seen in section II: Even if individual motions in
150 chaos are unpredictable, their long-term statistical properties in terms of probabilities are fully

151 predictable (Tél and Gruiz 2006; Tél, 2021), a feature corresponding to the essence of Lorenz's
152 predictability of the second kind (Lorenz, 1975).

153

154 REFERENCES NOT CITED IN THE MAIN TEXT

155

156 Keeling, C. D., Piper, S. C., Bacastow, R. B. , Wahlen, M., Whorf, T. P. , Heimann, M. ., Meijer,
157 H. A., 2001: Exchanges of atmospheric CO₂ and ¹³CO₂ with the terrestrial biosphere and
158 oceans from 1978 to 2000. I. Global aspects, SIO Reference Series, No. 01-06, Scripps
159 Institution of Oceanography, San Diego, 88 pages,
160 <http://escholarship.org/uc/item/09v319r9>.

161 Lorenz, E.N., 1975: Climate predictability. In: The Physical Basis of Climate and Climate
162 Modelling, WMO. GARP Publ. Ser. No. 16, 132-136. WMO, 265 pp.

163 Lucarini, V., Fraedrich, K. and Lunkeit, F., 2010: Thermodynamic analysis of snowball Earth
164 hysteresis experiment: Efficiency, entropy production and irreversibility. Q.J.R. Meteorol.
165 Soc., 136: 2-11. doi:10.1002/qj.543375

166 Lunkeit, F., Fraedrich, K., Jansen, H., Kirk, E., Kleidon, A., and Luksch, U., 2011: Planet
167 Simulator reference manual, available at [https://www.mi.uni-
168 hamburg.de/en/arbeitsgruppen/theoretische-meteorologie/modelle/plasim.html](https://www.mi.uni-hamburg.de/en/arbeitsgruppen/theoretische-meteorologie/modelle/plasim.html).

169 Maier-Reimer, E., Mikolajewicz, U., 1991: The Hamburg Large Scale Geostrophic Ocean
170 General Circulation Model(Cycle 1). Technical Report / Deutsches Klimarechenzentrum, 2.

171 Tél T., 2021: Chaos physics: what to teach in three lessons? Physics Education 56, 045002(8)

172 Vincze, M., Bozóki, T., Herein, M. et al., 2021: The Drake Passage opening from an
173 experimental fluid dynamics point of view. Sci Rep 11, 19951.
174 <https://doi.org/10.1038/s41598-021-99123-0>.

175

176

177

178

179